Formation of local moments on iron in alkali-metal hosts

M. E. McHenry
Materials Science and Technology Division, Los Alamos National Laboratory, Los Alamos, New Mexico 87545 and Department of Metallurgical Engineering and Materials Science, Carnegie Mellon University, Pittsburgh, Pennsylvania 15213

J. M. MacLaren
Theoretical Divsion, Los Alamos National Laboratory, Los Alamos, New Mexico 87545

D. D. Vvedensky* and M. E. Eberhart
Materials Science and Technology Division, Los Alamos National Laboratory, Los Alamos, New Mexico 87545

M. L. Prueitt
Information Services Divsion, Los Alamos National Laboratory, Los Alamos, New Mexico 87545
(Received 31 July 1989)

Spin-polarized, self-consistent-field, scattered-wave calculations have been performed on FeM_{14}, FeM_{26}, and $FeCa_{18}$ clusters (M = Li,Na,K,Rb) modeling local environments of an isolated Fe impurity in bcc (M) and fcc (Ca) alkali-metal hosts. No stable moment is observed for the Ca host, while a spin moment of $2\mu_B$ is seen for Fe in the Li host which grows to over $3\mu_B$ in the Rb host. Orbital moments are also likely to be important because of the extreme atomic nature of the Fe d states. We infer these moments by consideration of the calculated $3d^7$ ground state. A configuration of nearly $3d^7$ for the Fe atom is inferred for all the alkali-metal hosts. Moment trends are explained in terms of nearly vanishing s-d hybridization in Rb but increasing s-d hybridization up the column to Li.

The formation of local magnetic moments on transition-metal impurities in s- or (s-p)-band hosts is of continuing experimental[1,2] and theoretical interest.[3–5] Recently, the variety of host materials has been extended to include alkali metals in the pioneering work of Riegel and co-workers.[6,7] Study of local-moment formation in alkali metals is important because of the wide range of atomic volumes and free-electron densities that are accessible. Further, small observed crystal-field splittings allow for the possibility of orbital as well as spin contributions to the moment. In fact, an interpretation based on an ionic model[5] was used by Reigel to explain his data.[6] Finally, the complexity of moment formation in alkali-metal hosts is reduced because the dominant interactions between the host and impurity are (s-d)-like, with only small directional components (p-d, d-d) in the hybrid bonds. Recently, several first-principles techniques have dealt successfully with the local-moment problem. An embedded-atom or cluster method employed by Zeller *et al.*[8] uses a multiple-scattering Green's-function approach to treat coupling to an otherwise perfect host. The self-consistent-field scattered-wave (SCF SW) technique[9] treats free clusters, and for suitable problems can be faster computationally. This method has been applied to systems where the perturbations to electronic and magnetic structure are spatially localized and thus amenable to a cluster description. Exchange splittings and local moments calculated for octahedral (Mn)Cu,[10] icosahedral (Mn)Al,[11,12] and octahedral (Mn)Al (Ref. 12) show good agreement with experiment. Current experimental interest, as well as interesting theoretical concern in local-moment systems in alkali-metal hosts, has motivated this study.

It is by now well known that zero-temperature local moments, as addressed in the Kondo problem,[13] are compensated by antiferromagnetic coupling with the conduction electrons, so that the resulting ground state is a singlet.[14] Although features of this spin-compensation cloud are evident in the alkali-metal states in cluster calculations,[15] the details of the Kondo singlet remain, as many-body effects are not directly addressable by local-density calculations.

We have calculated the electronic structure of FeM_{14} and FeM_{26} (M = Li,Na,K,Rb) clusters modeling an impurity Fe atom in bcc alkali-metal hosts coordinated to second- and third-nearest neighbors, respectively. We also examined an $FeCa_{18}$ cluster representing fcc Ca to second-nearest neighbors. This system has interesting magnetic structure with a small local moment, in contrast to the first-column alkali-metal hosts. Redfern *et al.*[16] have recently commented that resolution of the utility of clusters to model impurity effects may be best addressed by observing convergence of the properties of interest with cluster size. In this work, convergence of the magnetic properties in cluster size was checked carefully. The similarity in the local-moment behavior of the Fe impurity in both the 15- and 27-atom clusters lead us to conclude that the bulklike behavior is reproduced by clusters which include up to the second-nearest-neighbor shell of atoms.

Computational details include the use of equilibrium alkali-metal lattice spacing for all clusters with the Fe impurity substituted on the central site. No relaxation of the host lattice is allowed. As a result, most of the hybridization and localization effects observed can be attributed to the large size differences between the alkali-metal atoms. This is consistent with the aims of the experimental work, which were to expressly explore the influence of these size effects on electronic structure. Relaxation effects, although very important in some systems,[17] are thought to be of lesser importance in the alkali-metal hosts because of the free-electron (nondirectional) nature of the host states, as well as the extremely weak bonding between impurity and host. We further justify our neglect of relaxation effects by noting, that, for alkali metals, relaxation does not occur to more than 0.5% at free surfaces.[18] Furthermore, the extreme changes in alkali-metal radii imply that this will be the dominant effect, with relaxation effects relegated to a comparatively minor role.

The touching-sphere muffin-tin approximation is used since it yields an unambiguous partitioning of space (as compared with overlapping spheres). The interstitial charge density complicates assignment of charge density to specific atomic sites. This is problematic for s and p electrons, but for the extremely localized d electrons this is seen to be less of a concern. The Janak-Moruzzi and Williams[19] local-spin-density-functional parameterization of the Hedin-Lundqvist[20] local-density functional has been employed. Choice of the local-density functional is known to have important ramifications on the local moment for alloy systems very close to the magnetic instability.[21] The magnetic moment at each atomic site is an extremely slowly converging property (slower than the eigenvalue and total-energy convergence, for example), due the small magnetic exchange-correlation energy as compared to the Coulomb energy. These calculations have been converged to values of $\Delta E_{\rm tot}/E_{\rm tot} < 10^{-6}$ in all cases and, consequently, moments are converged to four decimal places. We also allow for nonintegral occupation of the state(s) at the Fermi level and choose the configuration which yields the lowest total energy. This typically leads to increased mixing of the minority-band d states and the host s-p states at the Fermi level.

Table I summarizes the results of spin-polarized calculations on the previous described Fe alkali-metal clusters in terms of the spin density observed in the atomic impurity and alkali-metal muffin-tin spheres and on the outer sphere. These results indicate a sizable local moment on Fe in all hosts with the exception of Ca. The moment on the Fe site is seen to grow moving from a Li host to Na. K and Rb induce the largest moments and are nearly identical. These trends in the local moment are consistent with experimental findings.[7] The local spin moment on Fe in K and Rb is seen to converge to a value exceeding $3\mu_B$, indicating more than three unpaired spins on the iron site. In all cases the comparison of the summed atomic-site moments and the cluster moment lead us to infer that the uncounted intersphere regions are polarized antiferromagnetically with respect to the Fe moment. This is consistent with the observations of Moruzzi, Janak, and Williams[22] of the polarization of interstitial regions in spin-polarized muffin-tin band-structure calculations. Nearest-neighbor alkali-metal atoms also show small antiferromagnetic polarization with respect to the iron-impurity moment; the size of this moment is seen to increase upon moving down the alkali-metal column. The existence of slightly more than three unpaired spins on the Fe sites suggests a spin-angular-momentum quantum number S of nearly 1.5, which, in turn, agrees with an ionic Fe ground-state configuration of $3d^7$.

The inference of a $3d^7$ Fe configuration implies that there is some charge transfer from either the alkali-metal host or Fe s band to the Fe d states. An increase of approximately one electron, in the d-electron count, above the $3d^6$ atomic ground state, can be observed from the Fe muffin-tin d-electron count shown in Table I. This increased d-electron count is accompanied by a depletion of the Fe s band to a degree consistent with the Fe-alkali-metal electronegativity difference. Whereas the $3d^6$ configuration is the ground state for the positively charged Fe^{2+} ion, the $3d^7$ configuration is the ground state for the Fe^- ion and, thus, should eventually be favored in an extremely electropositive host. Electronegativity arguments suggest this configuration to be the one in which the minority-spin Fe d states would lie close in energy to the alkali-metal Fermi level.

TABLE I. Fe d-electron count and spin density, S (μ_B), breakdown for the indicated clusters. $M1$, $M2$, $M3$ and OTS refer to first, second, and third neighbors, and outer-sphere muffin-tin regions, respectively.

	Fe d	$S_{\rm Fe}$	S_{M1}	S_{M2}	S_{M3}	$S_{\rm OTS}$
$FeLi_{14}$	6.93	2.28	−0.04	0.02		0.05
$FeNa_{14}$	6.84	2.96	−0.10	0.05		0.00
FeK_{14}	6.85	3.17	−0.10	0.03		−0.09
$FeRb_{14}$	6.82	3.21	−0.11	0.04		−0.01
$FeCa_{18}$	7.37	0.00	0.00	0.00		0.00
$FeLi_{26}$	7.05	2.12	−0.03	0.01	0.00	−0.01
$FeNa_{26}$	7.18	2.61	−0.05	−0.11	0.00	−0.03
FeK_{26}	6.92	3.07	−0.06	0.06	−0.01	−0.01
$FeRb_{26}$	6.92	3.12	−0.03	0.00	0.04	−0.03

TABLE II. Fe character (%) on the majority (↑) and minority (↓) t_{2g} and e_g orbitals in FeM_{14} and FeM_{26} clusters.

	$1e_g\uparrow$	$1t_{2g}\uparrow$	$2e_g\uparrow$	$2t_{2g}\uparrow$	$1e_g\downarrow$	$1t_{2g}\downarrow$	$2e_g\downarrow$	$2t_{2g}\downarrow$
$FeLi_{14}$	88	89	7	5	43	50	48	39
$FeNa_{14}$	96	96	2	2	36	42	59	53
FeK_{14}	99	99	1	1	34	40	62	55
$FeRb_{14}$	99	99	1	1	34	39	62	57
$FeLi_{26}$	68	71	10	9	24	19	69	68
$FeNa_{26}$	90	85	4	4	7	11	85	80
FeK_{26}	98	98	1	1	4	4	85	85
$FeRb_{26}$	99	99	1	0	4	4	85	84

We believe that this charge transfer is not an artifact of the cluster geometry for three reasons. First, the magnitude of the charge transfer is virtually invariant in cluster size for a given alkali host, in 15- and 27-atom clusters, indicating that the calculations have converged to bulklike values by three coordination spheres. Second, the magnitude of the charge transfer to the Fe atom scales with the electronegativity difference between the Fe atom and the alkali metal, offering a more plausible argument for its origin. Finally, similar 27-atom clusters consisting of only alkali-metal atoms have been examined, for which insignificant charge transfer to the central-atom site is observed, as well as a bulklike partial density of states on this atom. For Fe in K or Rb the local moment can be explained in terms of an ideally localized Fe-impurity state with between approximately seven d electrons yielding the observed about three unpaired spins. In the case of Na and Li hosts, significant hybridization occurs between the Fe d states and the alkali-metal s states, subtracting from the number of polarizable d states and thus reducing the moment. It should also be noted that significant amounts of Ca d character are observed, whereas d contributions are minimal in the first-row alkali metals. For a Ca host, this s-d and d-d hybridization is so strong that it lowers the energy of the d resonance to 0.1 eV below the Fermi level, and no stable moment is formed.

Our conclusion of a $3d^7$ configuration differs from the explanation of Riegel results in terms of a $3d^6$ configuration. In an ionic picture, a $3d^7$ configuration has a total angular momentum J of 4.5, which can be inferred yielding an effective moment of $6.63\mu_B$, while an effective moment of $6.70\mu_B$ can be inferred for the $3d^6$ configuration ($J=4$). The 1% difference in these effective moments points to the extreme difficulty in experimentally ascertaining the ground state of Fe in these systems. Furthermore, it seems implausible that the $3d^6$ configuration usually observed for Fe in conjunction with electronegative ions should persist in electropositive environments. Our calculations do not expressly address the multiplet structure of the Fe atom, nor do any local-density-functional calculations. However, strong inferential arguments are now presented which support the contention of an ionic ground state ($3d^7$) for the Fe atom. These arguments include localization of the d states, vanishing s-d hybridization, and the absence of crystal-field splittings.

Trends in localization or hybridization are borne out in a consideration of the fraction of Fe character in the t_{2g} and e_g orbitals of these clusters, as shown in Table II. The t_{2g} and e_g orbitals are the only ones allowed by symmetry to contain central-atom Fe d character in octahedral symmetry. It can be seen that the majority-spin $1t_{2g}$ and $1e_g$ orbitals contain character nearly completely localized on the Fe site (and nearly totally d character). The minority band states, in turn, reflect the degree of hybridization with the alkali-metal states. Upon going

TABLE III. Exchange and crystal-field splittings (eV) for FeM_{14} and FeM_{26} clusters.

	Crystal-field splittings		Exchange splittings	
	$1t_{2g}\uparrow$-$1e_g\uparrow$	$2t_{2g}\downarrow$-$2e_g\downarrow$	$1t_{2g}\uparrow$-$2t_{2g}\downarrow$	$1e_g\uparrow$-$2e_g\downarrow$
$FeLi_{14}$	0.02	0.11	2.46	2.37
$FeNa_{14}$	0.02	0.03	2.61	2.66
FeK_{14}	0.01	0.02	2.63	2.66
$FeRb_{14}$	0.00	0.02	2.70	2.72
$FeLi_{26}$	0.04	0.20	1.93	1.78
$FeNa_{26}$	0.06	0.09	1.99	1.97
FeK_{26}	0.01	0.03	2.38	2.36
$FeRb_{26}$	0.01	0.01	2.43	2.42

from the 15-atom to the 27-atom cluster, the minority *d*-band width is seen to narrow significantly with most of the Fe character on the $2t_{2g}$ and $2e_g$ states, which represent the lowest unoccupied molecular-orbital state (LUMO) and the highest occupied molecular-orbital state (HOMO), respectively. This narrowing occurs predominantly because the second-shell alkali atoms have more complete coordination. The $2e_g$ state contains the two remaining Fe *d* electrons in the case of the K and Rb hosts, in which little hybridization with the host is observed.

The localization of the moment with alkali-metal hosts further down the column is further manifested in the spin-density plots of Fig. 1. This figure shows the total spin density as derived from the difference in the total charge density between the occupied spin-up and spin-down states for the $FeLi_{26}$ and FeK_{26} clusters in the (100) and (110) planes, respectively. This spin density is shown on a square grid scaled to the lattice constant. The spin density for $FeNa_{26}$ (not shown) exhibits localization intermediate to that of $LeLi_{26}$ and FeK_{26}. The $FeRb_{26}$ cluster is essentially similar to that of FeK_{26}. For the $FeLi_{26}$ cluster the spin density is more diffuse, reflective of the greater hybridization with the Li states, while the FeK_{26} cluster is considerably more localized, with little hybridization effects. These spin densities reflect zero-temperature occupancies. At finite temperatures the spin density for the FeK_{26} cluster is apt to look even more spherical since the small splitting between the $2t_{2g}$ (LUMO) and $2e_g$ (HOMO) states leads their contributions to the spin density to be increasingly indistinguishable.

Table III summarizes the trends in the crystal-field and exchange splittings in the clusters as estimated from pertinent eigenvalue differences. These excitation energies are more correctly calculated using Slater's[23] transition-state scheme. A comparison with transition-state-calculated values for the 27-atom Li cluster showed only small deviations from the values calculated from the difference in eigenvalues. However, given this approximation, as well as the finite-cluster geometries, more weight should be given to the trends in these numbers than to their absolute values. The crystal-field splitting for the majority-spin band is calculated as being the difference between the majority-band $1t_{2g}$ and $1e_g$ eigenvalues. For the minority band the $2t_{2g}$ and $2e_g$ difference is used since these states have the largest Fe character. The crystal-field splitting is seen to decrease by more than an order of magnitude in going from Li to the Rb host. This small crystal-field splitting for the K and Rb hosts is small enough to be consistent with an ionic picture and an unquenched local moment. The values of the crystal-field splittings in the K and Rb hosts are in good agreement with an upper bound of 0.03 eV, as determined by Riegel *et al.*[6]

In the case of a Li host, both the larger crystal-field splitting and the significant Fe-host hybridization suggest that orbital quenching of the moment should be significant. This coupled with the smaller spin moment implies a much smaller total moment for Fe in the Li host. Table III also shows the exchange splitting as es-

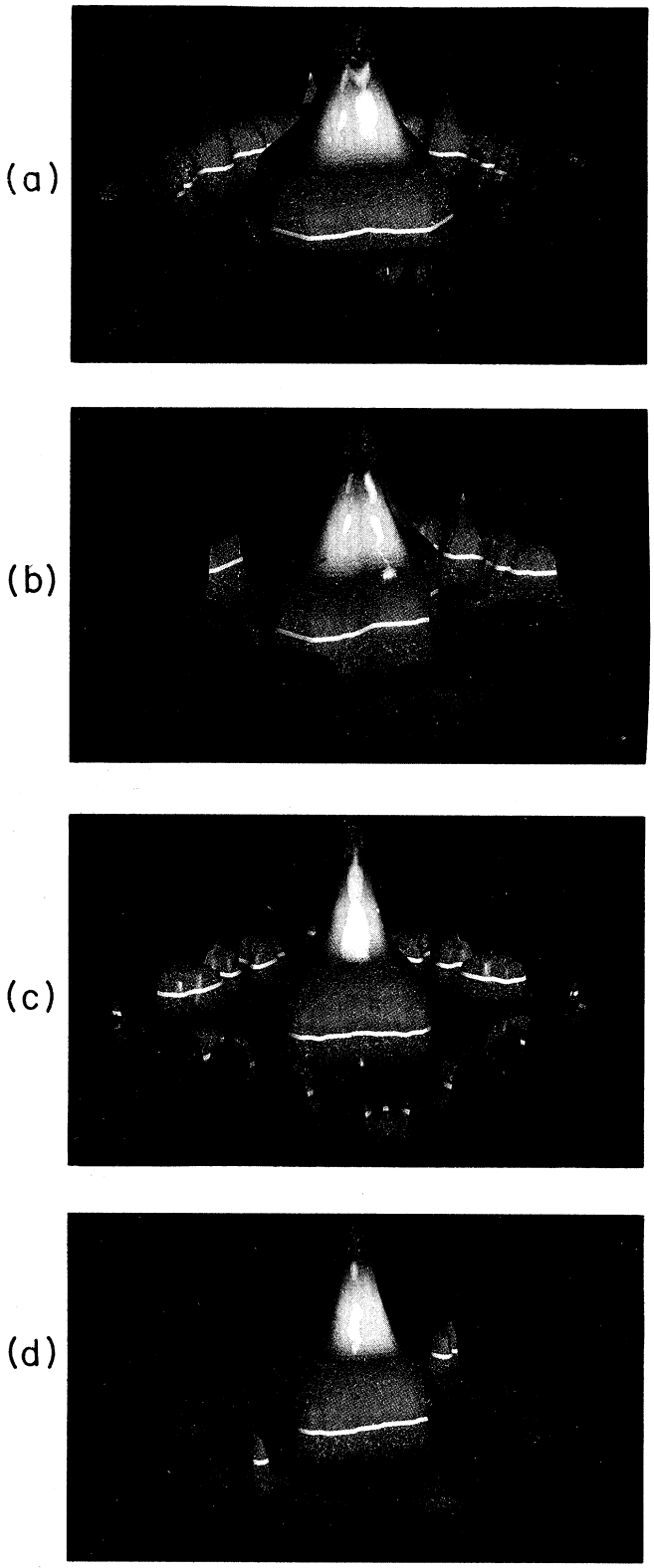

FIG. 1. Spin-density contour maps [plotted as $\mathrm{sgn}(\rho^{\uparrow}-\rho^{\downarrow})|\rho^{\uparrow}-\rho^{\downarrow}|^{[0,2]}$] for $FeLi_{26}$ and FeK_{26} clusters: (a) $FeLi_{26}$ (100) plane, (b) $FeLi_{26}$ (110), (c) FeK_{26} (100), and (d) FeK_{26} (110). These densities are plotted on a square grid scaled by the lattice constant.

timated by the $1t_{2g}$-$2t_{2g}$ and $1e_g$-$2e_g$ eigenvalue differences. The exchange splitting is seen to grow in going from the Li to the Rb host. The value of 2.5 eV is somewhat larger than that observed for Fe in a Cu host[10] in which a 2-eV exchange splitting was observed. In the Cu host, however, large crystal-field splittings (also on the order of 2 eV) were observed, signifying a quenched orbital-angular-momentum contribution. The large exchange splitting is consistent with the atomic nature of the Fe states.

In conclusion, a nearly $3d^7$ configuration is calculated for an Fe impurity in the hosts Li, Na, K, and Rb for both 15- and 27-atom clusters A spin moment of $3\mu_B$ consistent with this configuration is observed for K and Rb hosts. For Na and Li hosts the spin moment is reduced by increasingly more significant impurity-d–host (s-p)-hybridization effects. Vanishing crystal-field splittings and large exchange splittings for the polarized d states of the Fe impurity in K and Rb suggest the possibility of an unquenched (ionic) total angular momentum and, consequently, a large observed local moment. The smaller exchange splitting, significant crystal-field effects, and increasing hybridization upon going to Na and Li hosts suggest a more quenched moment, consistent with the experimental observations of a smaller effective moment in these hosts.[7]

This work was supported by the U.S. Department of Energy and in part by a NATO travel grant. Two of us (J.M.M.) and (M.E.M.) would like to thank Dr. H. Casey and MST6 for substantial support required for the completion of this work. Another (D.D.V.) would like to acknowledge the hospitality of the Materials Science and Technology Division at Los Alamos National Laboratory.

*Permanent address: The Blackett Laboratory, Imperial College, London SW7 2BZ, United Kingdom.

[1]D. K. Wohlleben and B. R. Coles, in *Magnetism,* edited by H. Suhl (Academic, New York, 1973), Vol. 5.
[2]G. Grüner, Adv. Phys. **23**, 941 (1974).
[3]P. W. Anderson, Phys. Rev. **124**, 41 (1961).
[4]J. Kondo, in *Solid State Physics,* edited by F. Seitz, D. Turnbull, and H. Ehrenreich (Academic, New York, 1969), Vol. 23, p. 183.
[5]L. L. Hirst, Phys. Kondens. Mater. **11**, 255 (1970); Z. Phys. **241**, 378 (1971).
[6]D. Riegel, H. J. Barth, L. Büerman, H. Haas, and Ch. Stenzel, Phys. Rev. Lett. **57**, 388 (1986).
[7]D. Riegel, L. Buerman, K. D. Gross, M. Luszik-Bhadra, and S. N. Mishraj, Phys. Rev. Lett. **61**, 2129 (1988).
[8]R. Zeller, R. Podloucki, and P. H. Dederichs, Z. Phys. B **38**, 201 (1980); R. Podloucki, R. Zeller, and P. H. Dederichs, Phys. Rev. B **22**, 5777 (1980); P. J. Braspenning, R. Zeller, A. Lodder, and P. H. Dederichs, *ibid.* **29**, 703 (1984).
[9]J. C. Slater and K. H. Johnson, Phys. Rev. B **5**, 844 (1972).
[10]D. D. Vvedensky, M. E. Eberhart, and M. E. McHenry, Phys. Rev. B **35**, 2061 (1988).
[11]M. E. McHenry, M. E. Eberhart, R. C. O'Handley, and K. H. Johnson, Phys. Rev. Lett. **56**, 81 (1988).
[12]M. E. McHenry, D. D. Vvedensky, M. E. Eberhart, and R. C. O'Handley, Phys. Rev. B **37**, 10 887 (1988).
[13]J. Kondo, Prog. Theor. Phys. **32**, 37 (1964).
[14]N. Andrei, Phys. Rev. Lett. **45**, 379 (1980).
[15]K. H. Johnson, D. D. Vvedensky, and R. P. Messmer, Phys. Rev. B **19**, 1519 (1979).
[16]F. R. Redfern, R. C. Chaney, and P. G. Rudolf, Phys. Rev. B **32**, 5023 (1985).
[17]N. Stefanou, P. J. Braspenning, R. Zeller, and P. H. Dederichs, Phys. Rev. B **36**, 6372 (1987).
[18]J. M. MacLaren, J. B. Pendry, P. J. Rous, G. A. Somorjai, M. A. Van Hove, and D. D. Vvedensky, *Surface Crystallographic Information Service* (Riedel, Dordrecht, 1987).
[19]J. F. Janak, V. L. Moruzzi, and A. R. Williams, Phys. Rev. B **12**, 1257 (1975).
[20]L. Hedin and B. I. Lundqvist, J. Phys. C **4**, 2064 (1971).
[21]S. Blugel, H. Akai, R. Zeller, and P. H. Dederichs, Phys. Rev. B **35**, 3271 (1987); J. M. MacLaren, M. E. McHenry, D. D. Vvedensky, and M. E. Eberhart (unpublished).
[22]V. L. Moruzzi, J. F. Janak, and A. R. Williams, *Calculated Electronic Properties of Metals* (Pergamon, New York, 1978).
[23]J. C. Slater, *Quantum Theory of Matter* (McGraw-Hill, New York, 1960).

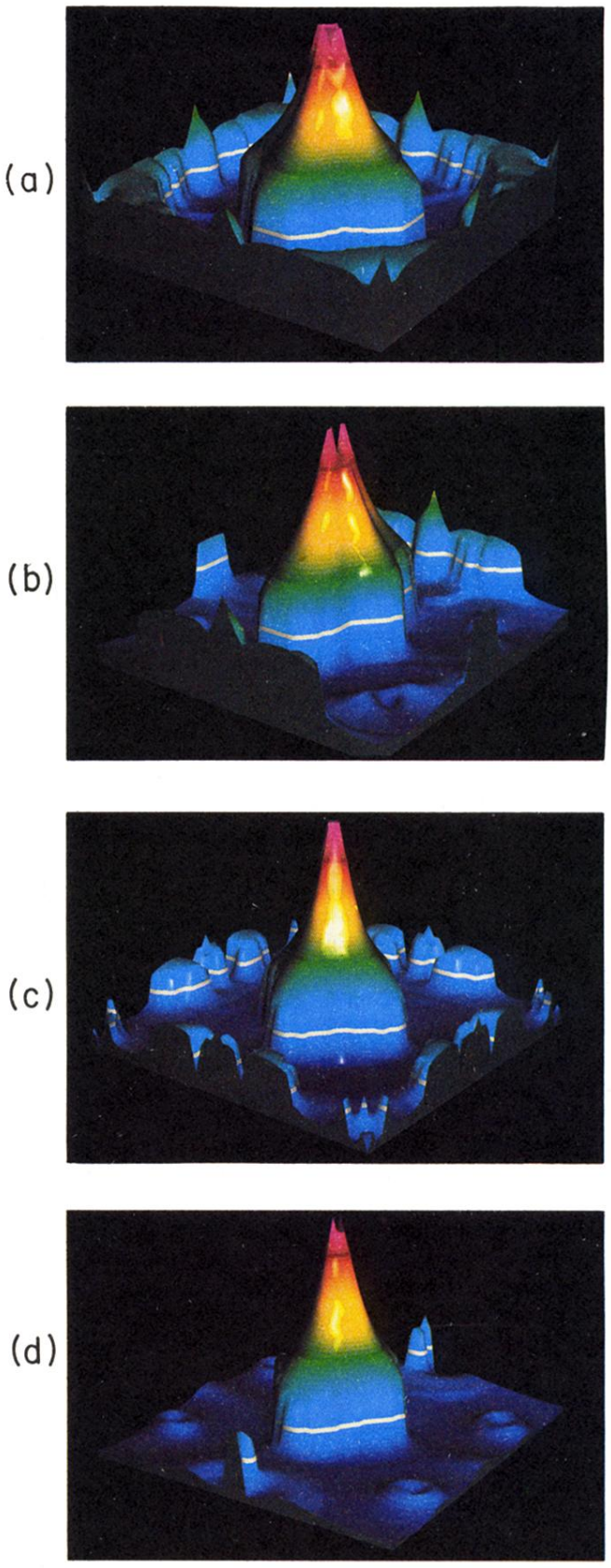

FIG. 1. Spin-density contour maps [plotted as $\mathrm{sgn}(\rho^{\uparrow}-\rho^{\downarrow})|\rho^{\uparrow}-\rho^{\downarrow}|^{0.2}$] for $FeLi_{26}$ and FeK_{26} clusters: (a) $FeLi_{26}$ (100) plane, (b) $FeLi_{26}$ (110), (c) FeK_{26} (100), and (d) FeK_{26} (110). These densities are plotted on a square grid scaled by the lattice constant.